Plant Mol Biol (2016) 92:675–687
DOI 10.1007/s11103-016-0538-8

Trichome patterning control involves TTG1 interaction with SPL transcription factors

Eugenia Ioannidi[1] · Stamatis Rigas[2] · Dikran Tsitsekian[2] · Gerasimos Daras[2] · Anastasios Alatzas[2] · Antonis Makris[3] · Georgia Tanou[1,5] · Anagnostis Argiriou[3] · Dimitrios Alexandrou[1] · Scott Poethig[4] · Polydefkis Hatzopoulos[2] · Angelos K. Kanellis[1]

Received: 24 March 2016 / Accepted: 29 August 2016 / Published online: 8 September 2016

Abstract Epidermal cell differentiation is a paramount and conserved process among plants. In *Arabidopsis*, a ternary complex formed by MYB, bHLH transcription factors and TTG1 modulates unicellular trichome morphogenesis. The formation of multicellular glandular trichomes of the xerophytic shrub *Cistus creticus* that accumulate labdane-type diterpenes, has attained much attention renowned for its medicinal properties. Here, we show that *C. creticus* TTG1 (CcTTG1) interacts with the SQUAMOSA PROMOTER BINDING PROTEIN-LIKE (SPLA/B) proteins, putative homologs of AtSPL4/5 that in turn interact with AtTTG1. These interactions occur between proteins from evolutionarily distant species supporting the conserved function of TTG1-SPL complex. Overexpression of *AtSPL4* and *AtSPL5* decreased the expression of *GLABRA2* (*AtGL2*), the major regulator of trichome morphogenesis, resulting in trichome reduction on the adaxial surface of cauline leaves, thereby illuminating the significance of TTG1-SPLs interactions in trichome formation control. *AtGL2* and *AtSPL4* have opposite expression patterns during early stages of leaf development. We postulate an antagonistic effect between SPLs and the heterogeneous MYB-bHLH factors binding to TTG1. Hence, the SPLs potentially rearrange the complex, attenuating its transcriptional activity to control trichome distribution.

Keywords *Arabidopsis* · *Cistus creticus* · Flavonoids · Root-hairs · Trichomes · *TTG1*/*GL2* pathway

Eugenia Ioannidi and Stamatis Rigas have contributed equally to this work.

Electronic supplementary material The online version of this article (doi:10.1007/s11103-016-0538-8) contains supplementary material, which is available to authorized users.

✉ Polydefkis Hatzopoulos
phat@aua.gr

✉ Angelos K. Kanellis
kanellis@pharm.auth.gr

[1] Group of Biotechnology of Pharmaceutical Plants, Laboratory of Pharmacognosy, Department of Pharmaceutical Sciences, Aristotle University of Thessaloniki, Thessaloniki, Greece

[2] Department of Biotechnology, Agricultural University of Athens, Iera Odos 75, 118 55 Athens, Greece

[3] Institute of Applied Biosciences, CERTH, Thessaloniki, Greece

[4] Department of Biology, University of Pennsylvania, Philadelphia, PA 19104-6313, USA

[5] Present address: Department of Agricultural Sciences, Aristotle University of Thessaloniki, 541 24 Thessaloniki, Greece

Introduction

Trichomes are highly differentiated epidermal cells of leaves representing physical and chemical barriers against environmental conditions. *Cistus creticus* is a dicotyledonous xerophytic shrub that grows in arid Mediterranean regions (Papaefthimiou et al. 2014). The multicellular glandular trichomes of *C. creticus* secrete "ladano", a resin enriched in labdane-type diterpenes, renowned for antimicrobial and cytotoxic properties (Falara et al. 2008, 2010).

In the model-species *Arabidopsis thaliana*, numerous genes and molecular regulatory networks have been identified to modulate epidermal cell differentiation (Hulskamp et al. 1999; Balkunde et al. 2010; Tominaga-Wada et al. 2011). The WD40 repeat protein TRANSPARENT TESTA

GLABRA1 (TTG1) is the common denominator of overlapping regulatory complexes that control cell fate and differentiation (Galway et al. 1994; Walker et al. 1999). In the root, TTG1 participates in the assembly of two distinct MYB-bHLH-WD40 (MBW) complexes that determine epidermal cell patterning (Schiefelbein et al. 2009, 2014). In non-hair cell files, TTG1 together with the MYB-domain protein WEREWOLF (WER) (Lee and Schiefelbein 1999), and two redundantly acting bHLHs, GLABRA3 (GL3) and ENHANCER OF GLABRA3 (EGL3) (Bernhardt et al. 2003, 2005; Payne et al. 2000; Simon et al. 2013), form a stable ternary WER-GL3/EGL3-TTG1 complex. This assembly positively regulates the expression of homeodomain-leucine-zipper (HD-Zip) transcription factor *GLABRA2* (*GL2*), which represses transcription of the downstream hair-cell promoting genes (Di Cristina et al. 1996; Masucci et al. 1996; Costa and Shaw 2006; Bruex et al. 2012). In the root-hair cells a set of small, one-repeat MYB proteins that lack transcriptional activation domains, including CAPRICE (CPC1), TRIPTYCHON (TRY), and ENHANCER OF TRY AND CPC1 (Kirik et al. 2004; Schellmann et al. 2002; Simon et al. 2007; Wada et al. 1997) competitively inhibit WER binding to the MBW complex (Tominaga et al. 2007; Ishida et al. 2008). This site-specific complex is not competent to stimulate *GL2* expression and thereby promotes root-hair cell fate.

In trichomes *GL2* is a positive regulator of epidermal differentiation (Masucci et al. 1996; Szymanski et al. 1998; Zhao et al. 2008). The MBW complex is still composed of TTG1, GL3 or EGL3 (Payne et al. 2000; Zhang et al. 2003) and the R2R3-MYB transcription factor GLABRA1 (GL1) (Kirik et al. 2005). Trichome development and regular spacing are controlled by TRY (Schellmann et al. 2002). TRY protein migrates to neighboring cells and competes GL1 binding leading to the formation of *GL2* inactive TRY-GL3/EGL3-TTG1 complex thereby inhibiting trichome fate (Schnittger et al. 1999; Esch et al. 2004).

The MBW transcriptional activation complex additionally modulates the late flavonoid biosynthetic genes. TTG1 associates with an MYB protein of the PRODUCTION OF ANTHOCYANIN PIGMENTS1 (PAP1)/PAP2/MYB113/MYB114 group, and a bHLH factor of the TRANSPARENT TESTA8 (TT8)/GL3/EGL3 group (Gonzalez et al. 2008; Zhang et al. 2003).

As the trichomes show diverse structural appearance and secondary metabolism, dissecting the interplay of the regulatory components involved in trichome patterning is stimulating. Here, we report that two CcSPLA/B proteins and their highly similar *Arabidopsis* homologues AtSPL4 and AtSPL5, physically interact with CcTTG1 and AtTTG1, respectively. Ectopic expression of miR156-resistant forms of *AtSPL4*/*5* genes in transgenic *Arabidopsis* lines diminished the function of the *TTG1*/*GL2* developmental pathway. Our results support the role of SPLs in trichome patterning control by potential modification of the MYB-bHLH-WD40 complex that is composed of heterogeneous protein partners.

Materials and methods

Plant materials and growth conditions

The *Arabidopsis ttg1* mutation in the *Landsberg erecta* (*Ler-0*) genetic background has a single base transition that introduces a premature termination codon resulting in C-terminal truncation (Walker et al. 1999). The *Arabidopsis* transgenic lines of *Columbia* (*Col-0*) ecotype background express the miR156-resistant forms of *SPLr4*/*5* genes under the control of the *CaMV35S* promoter (Wu and Poethig 2006). *Cistus creticus* plants were grown in pots under conditions as previously described (Falara et al. 2008). *Arabidopsis thaliana* and *Nicotiana benthamiana* plants were grown at 22 °C in a Fitotron (Weiss Gallenkamp; http://weiss-uk.com/) growth chamber with 100 µmol m^{-2} s^{-1} light intensity under 16 h light/8 h dark photoperiod. Morphometric analysis of epidermal cells performed as described (Rigas et al. 2009).

Isolation of Cc*TTG1*

A partial cDNA clone flanking the 5′ sequence of a WD40 repeat protein was identified from sequencing analysis of 2022 ESTs from a *C. creticus* cDNA library prepared from mRNA isolated from trichomes (Falara et al. 2008). The full-length cDNA, designated *CcTTG1*, was isolated by PCR amplification with a gene specific primer annealing at the 5′ of the EST clone using the Phusion HF polymerase (Finnzymes-Life technologies; https://www.lifetechnologies.com/) and gene specific primers (Supplementary Table 2). The 1023 bp product was cloned and fully sequenced.

Generation of transgenic *Arabidopsis thaliana* plant lines

CcTTG1 was cloned into the BamHI site of the pBI121 binary vector. The *Agrobacterium tumefaciens* strain C58C1 Rif^R carrying the non-oncogenic Ti plasmid pGV3101 was transformed by electroporation with the pBI121 construct (GenePulser II, Bio-Rad; http://www.bio-rad.com/). The construct was introduced into *ttg1* mutant background by vacuum infiltration as previously described (Rigas et al. 2009). T2 and T3 generation of transgenic plant lines selected on 40 mg l^{-1} kanamycin were assessed for capacity to complement *ttg1* pleiotropic defects.

Gene expression analysis

Total RNA was isolated using the phenol-sodium dodecyl sulfate (SDS) extraction method (Rigas et al. 2009). RNA concentrations were determined spectrophotometrically and verified by ethidium bromide staining on agarose gels. DNA was eliminated with RQ1 RNase-free DNase (Promega; http://worldwide.promega.com/). Reverse transcription (RT) was performed on 3 µg of total DNA-free RNA using Superscript II Reverse Transcriptase (Invitrogen-Life technologies; https://www.lifetechnologies.com/). RT-PCR gene expression analysis was performed using specific primers (Supplementary Table 3). The linear phase of semi-quantitative expression analysis was validated by preliminary experiments comparing the relative amounts of PCR products under low and high number of PCR amplification cycles. Quantitative gene expression analysis was performed by PikoReal 96 Real-Time PCR System (Thermo scientific; http://www.thermoscientific.com/) using the SYBR Select Master Mix (Applied Biosystems-Life technologies; https://www.lifetechnologies.com/) and calculated by the ΔΔCt method (Daras et al. 2009). Normalization of gene expression data was performed by using the housekeeping gene *glyceraldehyde-3-phosphate dehydrogenase* (*AtGAPDH*) as a reference. Total RNA isolation from *C. creticus* was performed as previously described (Pateraki and Kanellis 2004). RNA analysis by electrophoresis on denaturing formaldehyde agarose gels, Northern blotting onto nylon membranes (Schleicher and Schuell; http://www.schleicher-schuell.de/), hybridization and detection were performed as described (Sambrook et al. 1989).

Extraction and quantitative analysis of anthocyanins

Seedlings were grown under anthocyanin inductive conditions composed of high intensity light 300 µmol m^{-2} s^{-1} and increased supplemental carbon source 2% sucrose as previously described (Poustka et al. 2007). Anthocyanin content was determined as reported (Mehrtens et al. 2005).

Yeast-two-hybrid interactions

The *CcTTG1* cDNA was cloned into the BamHI/XhoI sites of pEG202 vector, containing the LexA DNA binding domain (BD) under the control of the *ADH* promoter. The *C. creticus* cDNA library of trichomes was constructed with 2 µg of total RNA using the SMART cDNA Library Construction Kit (Clontech; https://www.clontech.com/). The fragments of double stranded cDNA digested with SfiI restriction enzyme, larger than 500 bp, were cloned into the SfiI site of pJG4-5 plasmid, containing the *B42* transcriptional activation domain (AD) under the control of the *GAL1* promoter. *Saccharomyces cerevisiae* EGY48 yeast cells were co-transformed with BD and AD fusion constructs using the lithium acetate method (Gietz et al. 1992). Transformed yeast cells were tested on solid drop-out medium lacking histidine, tryptophan and leucine supplemented with 2% galactose/1% raffinose. To eliminate false positives yeast cells were tested on 2% glucose.

BiFC assays

The PCR products of *CcSPLA* and *CcSPLB* cDNAs amplified using the primers listed in Supplementary Table 2 were cloned into the SmaI site of pSPYCE vector to generate in-frame fusions with YFP^C (Walter et al. 2004). Likewise, *CcTTG1* was cloned into the SmaI site of pSPYNE vector generating in-frame fusion with YFP^N. For the isolation of *AtTTG1, AtSPL4* and *AtSPL5*, 5 µg of total DNA-free RNA isolated from *Arabidopsis* leaves were reverse transcribed and the full length cDNAs were PCR amplified using the gene specific primers shown in Supplementary Table 3. The PCR products were initially cloned into the SmaI site of pUC19 and then isolated with SalI/XmaI restriction enzymes. *AtTTG1* was inserted into the SalI/XmaI sites of pSPYNE vector, whereas *AtSPL4* and *AtSPL5* were introduced into the SalI/XmaI sites of pSPYCE vector, generating in-frame fusions with YFP^N and YFP^C, respectively. The basic leucine zipper (bZIP) transcription factor *bZIP63* cloned into pSPYCE and pSPYNE vectors was used as positive control due to homodimers formation in the nucleus (Walter et al. 2004). The constructs were inserted into *Agrobacterium tumefaciens* cells. Transient transfection of the split-YFP fusion constructs in *Nicotiana benthamiana* epidermal cells and live cell imaging were performed as previously described (Daras et al. 2014).

Bioinformatics

The software packages and online tools used in this study are shown in Supplementary Table 4.

Accession numbers

Sequence data from this article can be found in the EMBL/GenBank databases under accession numbers: *CcTTG1*: KT892927; *CcSPLA*: KU145276; *CcSPLB*: KU041720; *CcEF1a*: EF062868.

Results

Structural differences occur between CcTTG1 and AtTTG1

The leaves of *A. thaliana* are covered by unicellular non-glandular trichomes, whereas *C. creticus* (Supplementary

Fig. 1) has multicellular non-glandular and glandular trichomes, with the latter being the primary accumulation sites of "ladano" (Fig. 1a, b). To decipher the molecular mechanism that controls *C. creticus* epidermal cell differentiation to trichomes, the homolog of *TTG1* gene (Cc*TTG1*) was identified. Comparison of CcTTG1 deduced amino acid sequence with the *Arabidopsis* TTG1 (AtTTG1) homologue shows 77 % identity and 88 % similarity retaining a number of amino acid residues important for the three-dimensional conformation of the entire protein. CcTTG1 predicted to contain four WD40 repeat motifs ranging in length from 41 to 47 amino acids residues that perfectly match with the AtTTG1 motifs (Fig. 1c). The third motif (III), which is the longest, bears no proline residues contrary to the second (II) and fourth (IV), each having three prolines. However, the first (I) WD40 repeat motif of CcTTG1 consists of five prolines compared to the first motif of AtTTG1 that has eight prolines (Fig. 1c).

Phylogenetic analysis showed that CcTTG1 clusters together with TTG1-like WD40 proteins from dicotyledonous plants (Supplementary Fig. 2a; Supplementary Table 1). The *Brassicaceae* TTG1 homologs, including AtTTG1, group together consistent with the evolutionary relationships of these species (Supplementary Fig. 2a, b). These TTG1 homologs slightly deviated from CcTTG1, which is highly similar to the TTG1-like protein from cotton (*Gossypium hirsutum*), given that both species belong in the *Malvales* order.

Molecular models that project the structure of AtTTG1 and CcTTG1 predict distinctive structural differences as

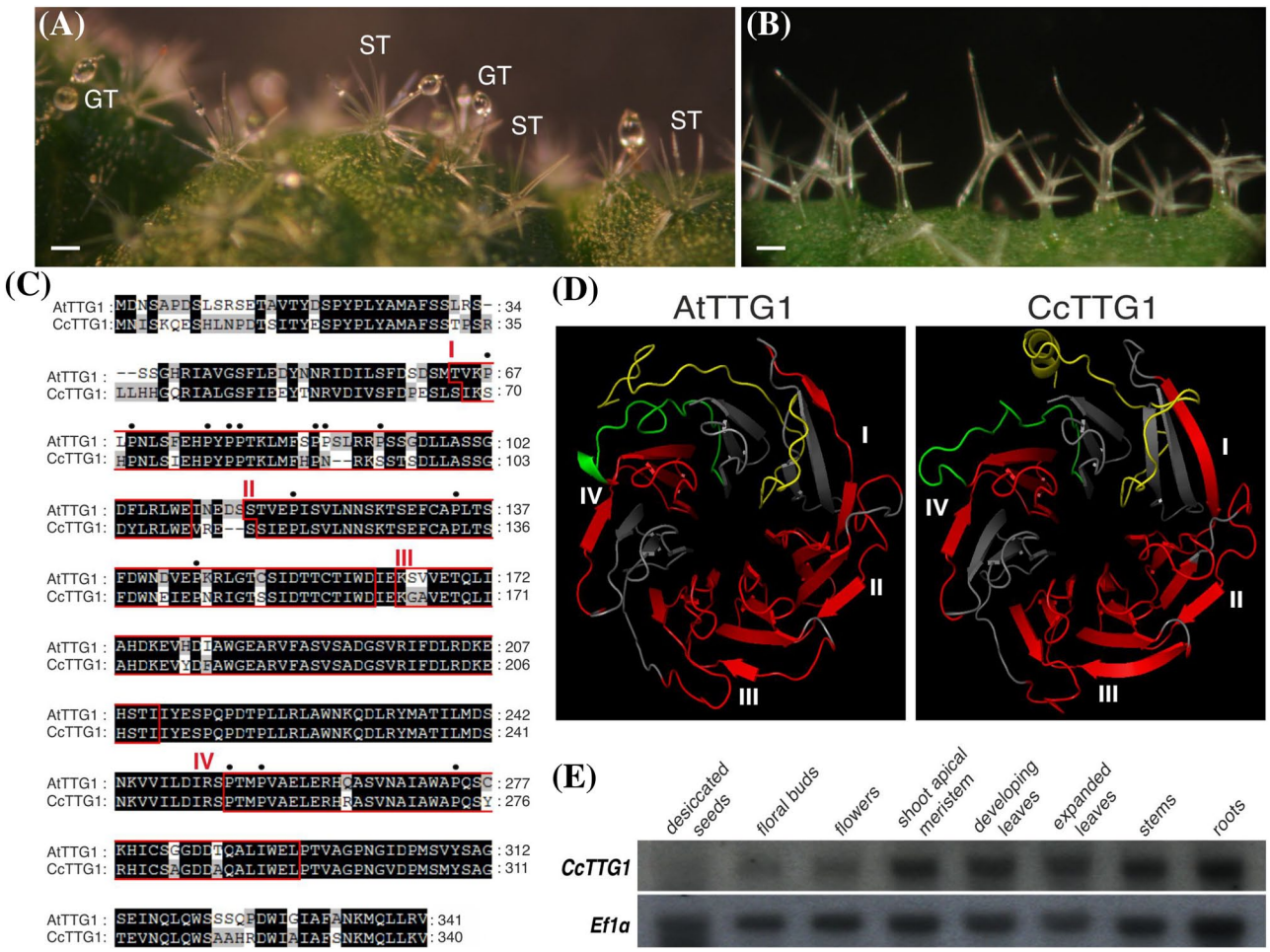

Fig. 1 Structural properties and expression profile of *CcTTG1*. **a** The leaves of *C. creticus* are covered by glandular trichomes (GT) and stellate trichomes (ST). *Scale bar* 100 µm. **b** In *Arabidopsis*, the leaf trichomes are unicellular epidermal hairs with a branched morphology. Scale bar, 100 µm. **c** Sequence comparison between the deduced amino acid sequences of *C. creticus* TTG1 (CcTTG1) and *A. thaliana* TTG1 (AtTTG1). *Dark shading* depicts identical amino acids, whereas *light grey shading* represents amino acid residues with similar physicochemical properties. *Boxed areas* (I-IV) indicate the conserved WD-repeats. The proline residues are marked with *dots*. **d** Comparative molecular modeling of CcTTG1 and AtTTG1 protein structure. The ribbon model distinguishes four highly conserved WD-repeats (*red*) from the most variable N- and C-terminal domains depicted in *yellow* and *green* color, respectively. **e** Northern blot analysis of *TTG1* expression in *C. creticus* tissues. The elongation factor 1a is used as loading control

the primary structure of the N- and C-terminal domains is variable between the two polypeptides (Fig. 1d). Moreover, the proline residues located within the WD40 repeat motifs possibly determine the periodicity and regularity of blade folding that drives the formation of the circular propeller structure. Hence, CcTTG1 compared to AtTTG1 has subtle structural differences, albeit the typical TTG1-like WD40 protein conformation, that potentially could reflect the functional interplay with different regulatory components.

Expression profile analysis revealed that the *CcTTG1* transcript is present in all tested organs (Fig. 1e), in agreement with previous reports in *Arabidopsis* (Walker et al. 1999). Nevertheless, in *C. creticus, TTG1* appears to have a prominent expression in organs bearing high trichome and root-hair content including leaves, stems and roots.

CcTTG1 structural differences determine its functional capacity to control *Arabidopsis* trichome patterning

To test whether these subtle structural differences are important for the capacity of CcTTG1 to complement the functional impairments of *ttg1*, the *Arabidopsis* mutants were transformed with the *CcTTG1* homologue (Supplementary Fig. 3). Phenotypic analysis of transgenic *Arabidopsis ttg1* plants, referred as *CcTTG1* transgenic plants, revealed a partial functional competence of *CcTTG1* to restore trichome patterning (Fig. 2a). The number of trichomes on the cauline leaves of transgenic plants were significantly reduced by approximately one-third (Fig. 2b). However, the ectopic root-hair patterning of *ttg1* mutant was fully restored (Fig. 2c). The epidermal cells differentiated to root-hairs were indistinguishable from the wild-type seedlings (Fig. 2d). Hence, the inability of *CcTTG1* to fully complement the *glabrous* phenotype of *ttg1* plants could be attributed to the subtle, nevertheless critical differences of CcTTG1 conformation and to the heterogeneity of the protein interaction partners within the *Arabidopsis* leaf epidermal cells that likely result in the formation of a rather unstable ternary transcriptional active complex. However, the results show that *CcTTG1* is able to trigger the developmental cascade of *Arabidopsis* genes towards epidermal cell differentiation.

Additionally, TTG1 forms a regulatory complex with MYB-bHLH transcription factors activating the expression of the late genes involved in the biosynthetic pathway of flavonoids. These genes result in the accumulation of anthocyanins and proanthocyanidins (PAs) in vegetative tissues and the seed coat, respectively (Li 2014; Xu et al. 2015). To assess the ability of *CcTTG1* to complement the biosynthesis of flavonoids, the transgenic plant lines were grown under anthocyanin inductive conditions (Poustka et al. 2007). The biosynthesis of purple anthocyanins was restored at the junction between hypocotyl and cotyledons of the trangenic plants, whereas the yellow color of *ttg1* seeds turned brown due to the accumulation of oxidized proanthocyanidins (Fig. 2e, f). To evaluate the reconstitution of the metabolic pathway, measurements of anthocyanins accumulation were made. The data pinpoint that *CcTTG1* completely repaired the defects in anthocyanins biosynthesis, restoring their accumulation to wild-type levels (Fig. 2g, h). On the basis of these observations, the *TTG1* homolog of *C. creticus* forms a stable ternary complex compensating the metabolic disorders of *Arabidopsis ttg1* plants in different tissues.

CcTTG1 activates the *GL2* regulator implicated in epidermal cell differentiation of *Arabidopsis* seedlings

The *GL2* transcription factor is, among other genes, a downstream molecular target of the MBW complex (Masucci et al. 1996; Szymanski et al. 1998; Zhao et al. 2008). Hence, the functional competence of *CcTTG1* to activate *GL2* expression in *ttg1* background was validated. As *ttg1* is a nonsense mutation resulting in a premature stop codon, the expression level of *AtTTG1* in the transgenic lines was similar to that in wild-type seedlings (Fig. 3a). Contrary to *ttg1* seedlings, the ectopic expression of *CcTTG1* highly increased the abundance of *AtGL2* (Fig. 3a). Quantification analysis confirmed that the elevated expression level of *AtGL2* was identical to wild-type seedlings and significantly different from *ttg1* seedlings (Fig. 3b). Hence, in the seedlings that have cotyledons without trichomes, *CcTTG1* fully restored the *AtGL2* expression, a negative regulator of root-hair morphogenesis, in consistency with the reduction of the root-hair density observed in the transgenic lines (Fig. 2c, d). By using RNA from the first pair of cauline leaf primordia, the expression of the trichome positive regulator *AtGL2* is also activated in *CcTTG1* transgenic lines (Fig. 3c). However, the expression level of *AtGL2* was, on average, equal to half of that observed in wild-type cauline leaves (Fig. 3d). This expression pattern coincides with the reduced number of trichomes observed on the cauline leaves of *CcTTG1* transgenic plants (Fig. 2a, b). These results provide evidence for reconstitution of the *TTG1*/*GL2* developmental pathway upon heterologous expression of *CcTTG1* in *Arabidopsis ttg1* seedlings and suggest that partial restoration of *GL2* expression on cauline leaves trichomes is likely attributed to structural differences of CcTTG1 and to the heterogeneity of the protein interaction partners.

CcSPL transcriptional activators interact with CcTTG1 in the nucleus

Given the central role of TTG1 in multiple aspects of cell differentiation and metabolism, a screen was performed to identify protein interaction partners by the yeast two-hybrid assay. Using CcTTG1 as bait a cDNA library prepared from

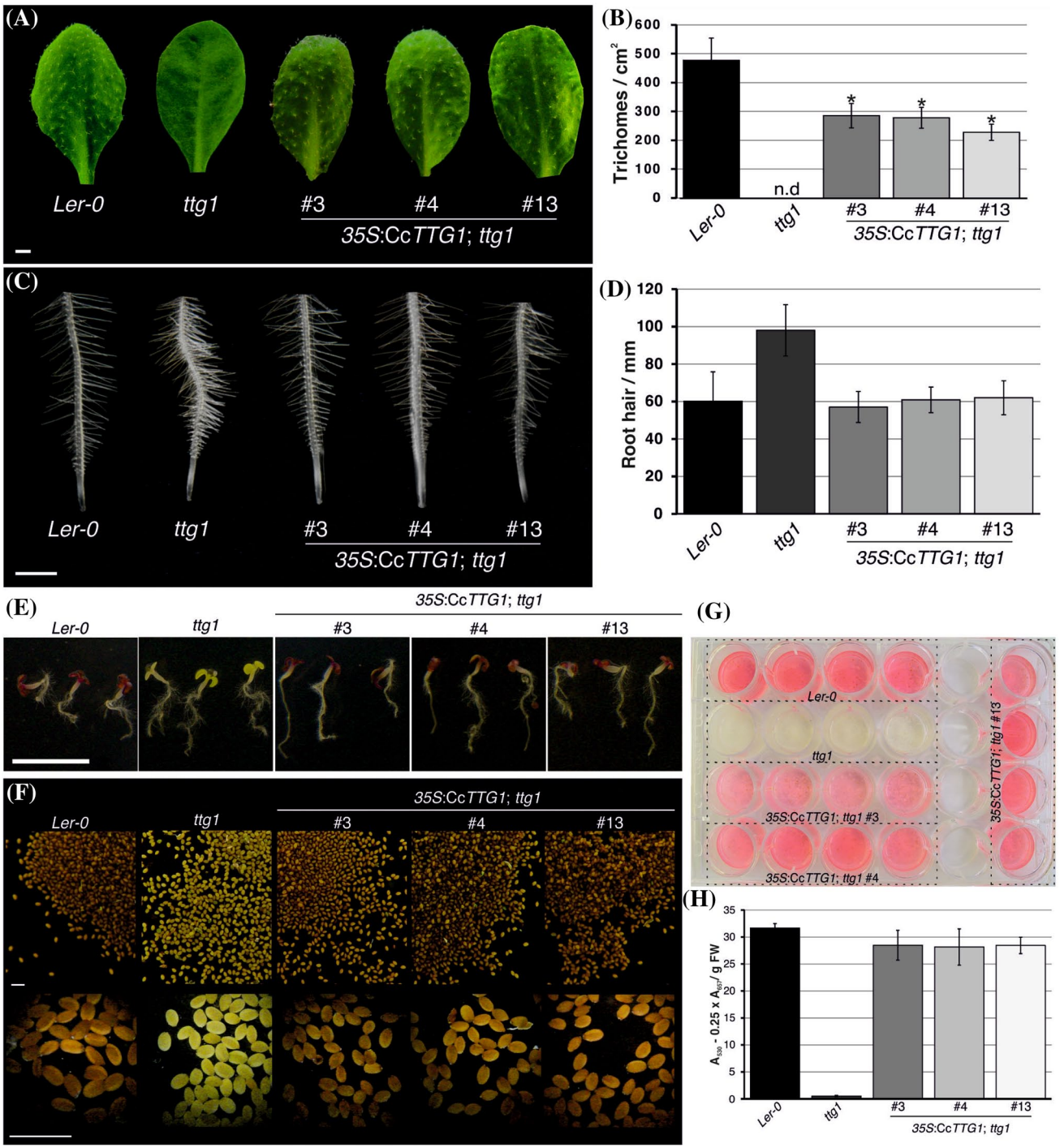

Fig. 2 *CcTTG1* reflects the heterogeneity of the transcription factors controlling *Arabidopsis* trichome formation. **a** *CcTTG1* partially complements the *glabrous* phenotype restoring the formation of trichomes in cauline leaves. *Scale bar* represents 1 mm. **b** Trichome density calculated by the analysis of 15 distinct cauline leaves from each transgenic line. *Asterisks* indicate significant difference between the wild-type plants (*Ler-0*) and transgenic lines ($P < 0.01$; Student's *t* test). **c** Primary root architecture of vertically grown 5-days-old seedlings. *Scale bar* represents 1 mm. **d** Root-hair density of 5-days-old seedlings calculated by the analysis of 20 primary roots from each transgenic line. No significant difference was found between the wild-type plants (*Ler-0*) and transgenic lines ($P < 0.01$; Student's *t* test). **e** At the junction between hypocotyl and cotyledons of 9-days old seedlings the accumulation of anthocyanins is restored by Cc*TTG1*. *Scale bar* represents 5 mm. **f** *CcTTG1* complements the *transparent testa* phenotype restoring the accumulation of proanthocyanidins in the seed coat mucilage. *Upper panel, Scale bar* represents 1 mm. *Lower panel, Scale bar* represents 1 mm. **g** Extracts of anthocyanins from 9-days old seedlings. **h** Quantitative analysis of anthocyanin content. Values are means ± standard error ($n = 4$) normalized per g of fresh weight. No significant difference was found between the wild-type plants (*Ler-0*) and transgenic lines ($P < 0.01$; Student's *t* test)

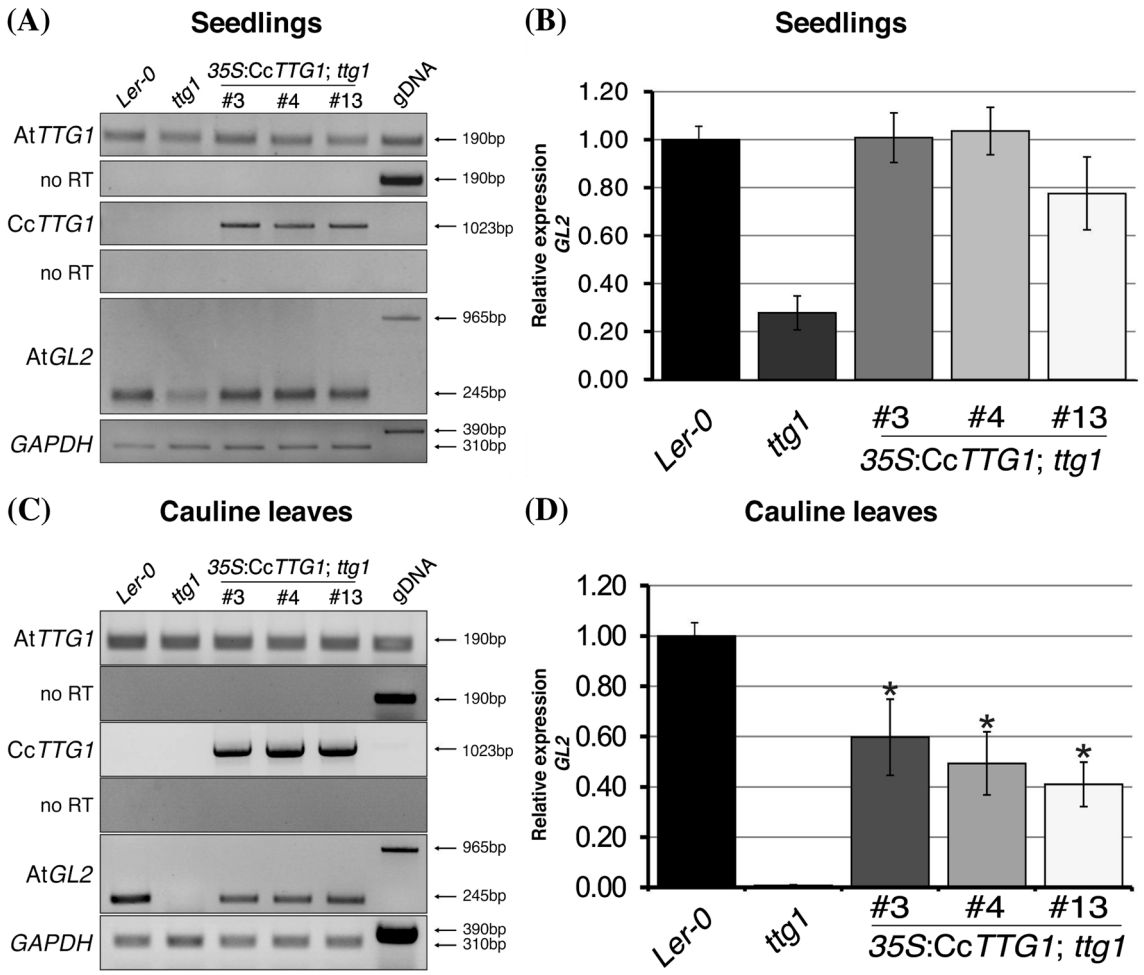

Fig. 3 *CcTTG1* restores the expression of *AtGL2* key regulator of epidermal cell patterning in *Arabidopsis ttg1* mutant background. Expression levels of *AtTTG1, AtGL2* and *AtGAPDH* genes by semi-quantitative (**a, c**) and Real-time (**b, d**) RT-PCR analysis. No RT reactions indicate that the RNA samples are free from genomic DNA contamination. Values are means ± standard error for fold changes relative to wild-type ecotype *Ler-0* detected by quantitative RT-PCR of three biological replicates, each analyzed in triplicate. In seedlings (**b**), no significant difference was found between the wild-type plants (*Ler-0*) and transgenic lines ($P < 0.01$; Student's *t* test). In cauline leaves (**d**), the *asterisks* indicate significant difference between the wild-type plants (*Ler-0*) and transgenic lines ($P < 0.01$; Student's *t* test)

C. creticus trichomes was screened. Two SPL transcriptional activators, hereafter called CcSPLA/B, interacted with CcTTG1 (Fig. 4a). Consistent with the stability of CcSPLA/B-CcTTG1 interactions, the yeast cells failed to grow in the presence of glucose that repressed the transcription of the galactose regulatory system. To confirm these interactions *in planta* the bimolecular fluorescence complementation (BiFC) assay was applied in transiently transfected *Nicotiana benthamiana* epidermal cells. Reconstituted fluorescence was detected upon interaction of CcTTG1 with either CcSPLA or CcSPLB and localized exclusively in the nucleus of the transfected cells (Fig. 4b), confirming that CcSPLA/B directly bind to CcTTG1 in vivo.

Phylogenetic analysis revealed that CcSPLA/B belong in the group of the miR156-targeted SPL transcription factors containing 11 members out of totally 17 SPL proteins encoded by the *Arabidopsis* genome (Xing et al. 2010). CcSPLA/B share a high level of protein similarity with particularly three miR156-targeted AtSPL3/4/5 factors (Supplementary Fig. 4a). Phylogenetic analysis revealed that CcSPLA/B and their *Arabidopsis* homologs AtSPL3/4/5 cluster together and they are clearly separated from the members of the AtSPL9 subfamily (Supplementary Fig. 4b). Furthermore, the identity of CcSPLA with AtSPL4 and AtSPL5 is 46 and 45%, respectively, whereas this identity with AtSPL9 decreases to 18%. Likewise, the identity between of CcSPLB with AtSPL4 and AtSPL5 is 35 and 37%, respectively, whereas this identity with AtSPL9 decreases to 15%. As the gaps upon the protein alignment between CcSPLA/B and AtSPL9 increase dramatically, the homologs of CcSPLA/B, SPL4 and SPL5, were selected as candidates to interact with TTG1. To determine whether this interaction is conserved among plant species, BiFC assays were performed using the *Arabidopsis* AtSPL4/5 homolog proteins. The fluorescent signal was also

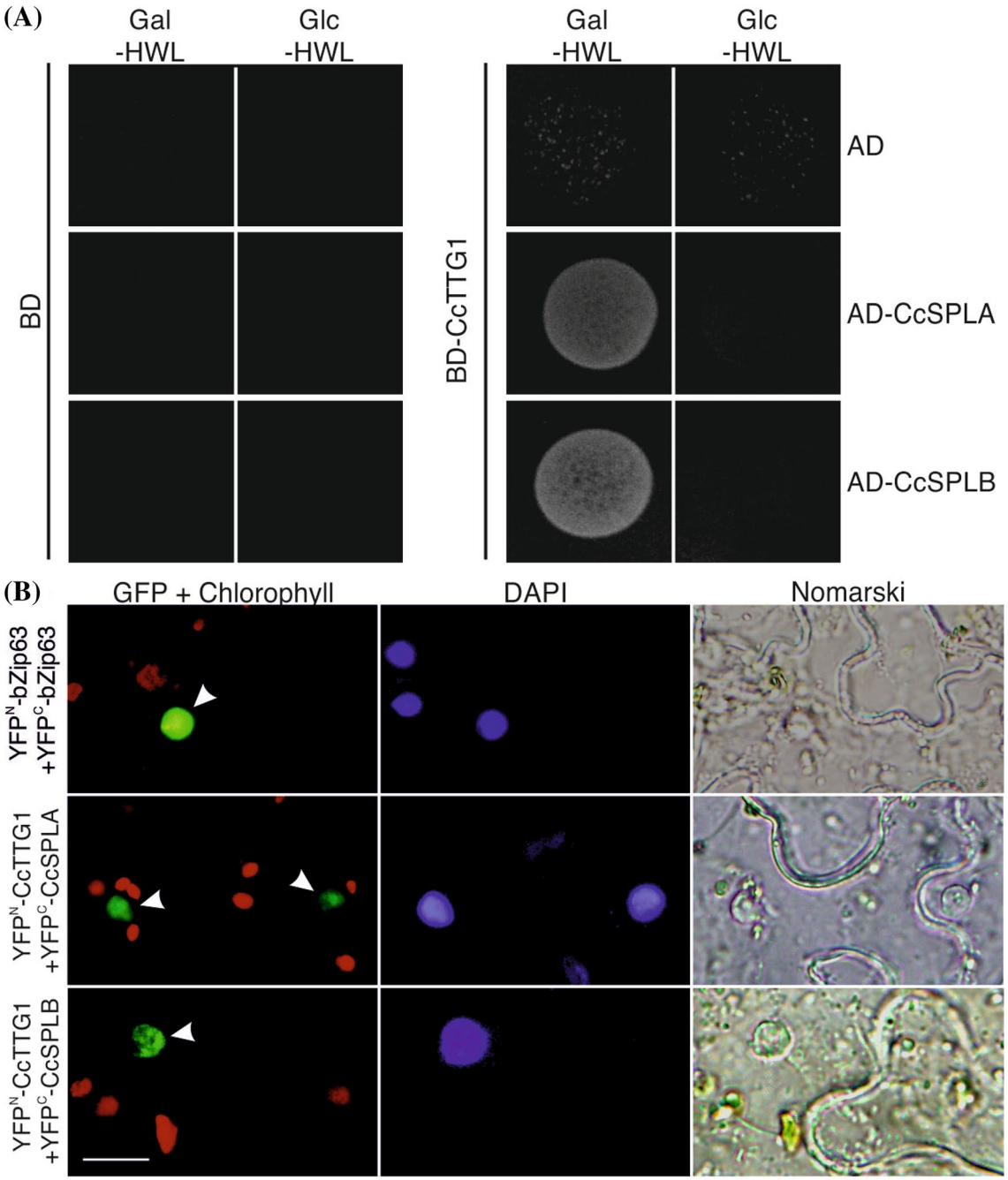

Fig. 4 Identification of CcTTG1 interaction partners. **a** CcSPLA/B bind to CcTTG1 in yeast. Yeast cells were co-transformed with combinations of binding domain (BD) and activation domain (AD) fusion constructs as indicated. Transformed yeast cells were grown on synthetic drop out (SD) selection plates lacking histidine, tryptophan and leucine (−HWL) in the presence of galactose (Gal) supplemented with raffinose or glucose (Glc). The pJG4-5 (AD) with pEG202 (BD), and the AD-CcSPLA/B fusions expressed with the BD alone were used as negative controls. **b** BiFC analysis of CcTTG1 interactions in the nucleus of transiently transfected *Nicotiana benthamiana* epidermal cells. bZIP63 that forms homodimers in the nucleus was used as positive control. *Green fluorescence* indicates the direct protein–protein interactions (*arrowheads*) between CcTTG1 and CcSPLA/B. *Red fluorescence* corresponds to chloroplasts due to chlorophyll auto-fluorescence. DAPI staining (5 μg mL^{-1}) was used for visualization of the nuclei (*middle* panel). *Scale bar* represents 50 μm

evident upon the interaction *in planta* of AtTTG1 with the AtSPL4 and AtSPL5 counterparts (Supplementary Fig. 4c). The nuclear localization pattern supports the conclusion that the in vivo binding between TTG1 and SPLs is conserved among evolutionary distant plant species (Supplementary Fig. 2b) revealing its importance in biological processes.

Although AtTTG1 has no obvious nuclear localization signal (NLS; Walker et al. 1999), the protein is present

in both the nucleus and the cytoplasm (Zhao et al. 2008; Balkunde et al. 2011; Cheng et al. 2014). The most plausible hypothesis is that TTG1 is not transported to the nucleus but the protein interacting factors promote its nuclear localization (Zhao et al. 2008; Balkunde et al. 2011). Unlike AtTTG1, the AtSPL4/5 proteins contain a bipartite NLS that overlaps with the highly conserved SBP-domain of 76 amino acids (Birkenbihl et al. 2005), which is shown in Supplementary Fig. 4a. The SBP-domain has been reported to bind specifically to GTAC core motifs of *Arabidopsis* promoters (Birkenbihl et al. 2005; Wang and Wang 2015) and therefore may be involved in the nuclear localization of the AtTTG1-AtSPL4/5 complex (Supplementary Fig. 4c). In silico analysis of CcTTG1 sequence failed to predict any putative NLS, whereas CcSPLA/B have a putative NLS overlapping with the highly conserved SBP-domain (Supplementary Fig. 4a) most likely involved in the CcSPLA/B-CcTTG1 complex nuclear translocation. Like their *Arabidopsis* homologs, the protein domains except the SBP-domain of CcSPLs are highly variable. Based on this insight, CcSPLA/B in terms of physical interaction with CcTTG1 likely followed a conserved evolutionary path to modulate specific TTG1-dependent biological processes.

SPL4/5 interfere in vivo with the regulation of MBW complex transcriptional activity

Our results support the notion that TTG1 is recruited by the SPL factors and thereby rearranges the MBW complex. We tend, therefore, to favor the hypothesis that elevated levels of SPLs may retract TTG1 and diminish the transcriptional activity of the MBW complex, causing defects reminiscent to *ttg1*-like phenotypes. To validate this hypothesis, we used *A. thaliana* transgenic plants overexpressing the *SPLr4/5* miR156-resistant (Wu and Poethig 2006) gene homologs of *CcSPLA/B* (Supplementary Fig. 4b). The stability of *SPL4/5* mRNAs against miR156 accelerates vegetative-to-reproductive phase transition promoting flowering by direct activation of *LEAFY, FRUITFULL* and *APETALA1* (Wu and Poethig 2006; Wu et al. 2009; Yamaguchi et al. 2009; Wang and Wang 2015). Our results confirmed that the high abundance of SPLr4/5 is tightly coupled with rapid entrance into the reproductive stage (Supplementary Fig. 5). The overexpressing *SPLr4/5* lines affected a broad range of developmental processes including leaf morphology and lamina area (Fig. 5a, b). Interestingly, while the trichome pattern was evident, the number of trichomes on the adaxial surface of cauline leaves was reduced to approximately half upon elevation of SPL4/5 levels (Fig. 5c). Given that TTG1 interacts with SLP4/5 in both species, this phenotypic defect provides strong evidence that elevated SPL4/5 levels recruit TTG1, and therefore interfere with the stability of the MBW complex mimicking the *ttg1*-like trichome disorder.

To confirm that SPL4/5 attenuate the transcriptional activity of MBW complex, the expression of *GL2* was monitored. RNA was isolated from the first pair of cauline leaf primordia when the plants were bolting, immediately after entering into the reproductive stage (Supplementary Fig. 5). Upon ectopic expression of *SPLr4* and *SPLr5*, the levels of *GL2* expression were decreased, whereas the expression of *TTG1* remained constant (Fig. 5d). Quantification analysis revealed that *GL2* expression was significantly reduced to approximately half and one-third in *SPLr4* and *SPLr5* plants, respectively (Fig. 5e), corroborating the phenotypic analysis (Fig. 5a). Moreover, in the first pair of cauline leaf primordia of *SPLr4* and *SPLr5* plants, the expression of trichome repressors *TRICHOMELESS1* (*TCL1*) and *TRY* was moderately increased (Fig. 5e). Unlike the trichome patterning phenotype, ectopic expression of miR156-resistant *SPL4/5* genes failed to reveal any evident defects associated with other TTG1-dependent biological processes. The root-hair patterning was not affected and *AtGL2* expression pattern was similar to *Col-0* seedlings (Supplementary Fig. 6). Likewise, the ectopic expression of *SPL4/5* had no effect on flavonoid biosynthesis (Supplementary Fig. 7). Taken together, these results provide conclusive evidence that the trichome patterning observed during overexpression of *SPL4/5* genes coincides with the decreased levels of *GL2* expression.

Discussion

Trichomes are differentiated epidermal cells that vary considerably between plants. Trichomes protect against insects, herbivores and UV radiation, control the temperature of leaf surface and prevent excessive transpiration (Johnson 1975; Balkunde et al. 2010). TTG1, a WD-repeat protein, forms a ternary complex together with R2R3-MYB and bHLH transcription factors, necessary for the expression of genes promoting trichome formation including *GL2* (Payne et al. 2000; Zhang et al. 2003; Kirik et al. 2005). Despite trichome formation, the interacting transcription factors form with TTG1 distinct MBW complexes that act as regulatory hubs controlling root-hair morphogenesis or flavonoids biosynthesis. In *ttg1* mutants, the formation of these MBW complexes is hindered, which prevents trichome formation causing the *glabrous* phenotype, promotes ectopic root-hair morphogenesis, and disrupts the biosynthesis of anthocyanins in vegetative tissues and proanthocyanidins in the seed coat mucilage resulting in the *transparent testa* phenotype (Galway et al. 1994; Walker et al. 1999).

Herein we demonstrate that similar to its *Arabidopsis* counterpart, the CcTTG1 polypeptide bears four WD40 repeat motifs, albeit the first repeat has five proline residues instead of eight. These distinctive differences together

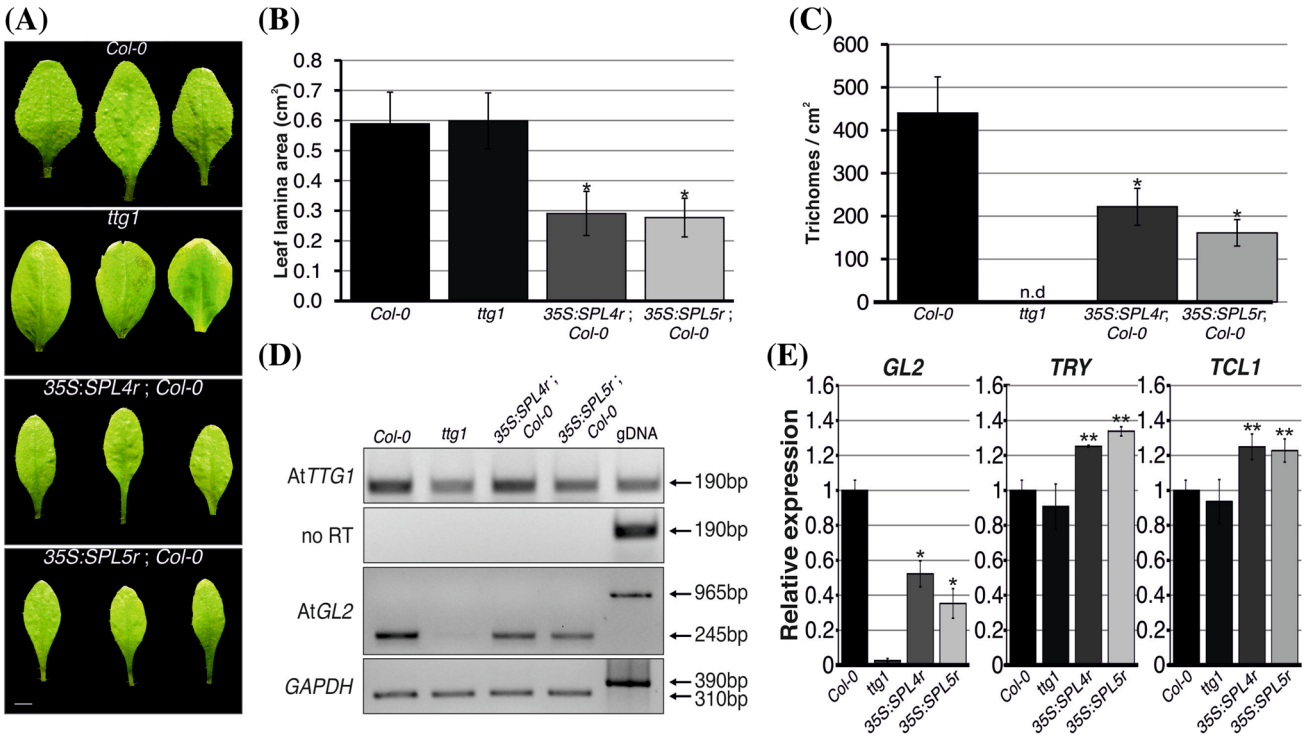

Fig. 5 Elevated *SPL4/5* levels accelerate vegetative-to-reproductive phase transition and reduce trichome density through *GL2* down-regulation. **a** and **b** Rapid phase transition modifies leaf morphology and leaf lamina geometry (n = 8). Scale bar represents 2 mm. **c** Trichome density per leaf lamina area on the adaxial surface of cauline leaves is reduced (n = 8). **d** and **e** Expression of the trichome inducer *GL2* or trichome repressors *TCL1* and *TRY* in the first pair of cauline leaf primordia. Relative gene expression levels by semi-quantitative (**d**) and real-time (**e**) RT-PCR analysis. No RT reactions indicate that the RNA samples are free from genomic DNA contamination. Values are means ± standard error for fold changes relative to wild-type ecotype *Col-0* detected by quantitative RT–PCR of three biological replicates, each analyzed in triplicate. Student's *t* test was used to indicate significant difference between the wild-type plants (*Col-0*) and the *SPLr4/5*-overexpressor lines at $P < 0.01$ (single *asterisks*) or $P < 0.05$ (double *asterisks*)

with the slightly variable N- and C-terminal domains most likely reflect the evolutionary distance between *C. creticus* and *A. thaliana*. It is therefore reasonable to assume that the structural differences modify the circular propeller core structure of CcTTG1 compared to AtTTG1 that partially affects the docking of heterogeneous *Arabidopsis* MYB and bHLH protein interaction partners in the trichome forming cells. Consequently, *CcTTG1* fully complemented the root-hair and flavonoid phenotype of *Arabidopsis ttg1* mutant, whereas resulted in hemi-complementation of the *glabrous* phenotypic defect. Hence, MBW complex integrity efficiently activates the expression of downstream regulatory genes that control root-hair formation and flavonoid biosynthesis contrary to the MBW complex formed in trichomes that is less active but still efficient. Identification of *CcTTG1* and its functional role in *Arabidopsis* gives an interesting twist to comprehend the molecular switch that controls trichome morphogenesis coupled with the accumulation of secondary metabolites in medicinal plants.

While in the absence of TTG1 the ectopic expression of the heterogeneous MYB and bHLH factors activate the downstream regulatory pathways, the presence of TTG1 is crucial stabilizing the ternary transcriptional complex (Baudry et al. 2004; Li 2014; Xu et al. 2015). Our results show that miR156-targeted SPL transcription factors bind to TTG1 attenuating the transcriptional activity of MBW complex, thus causing trichome reduction. A subset of 11 SPLs is targeted by miR156 (Xing et al. 2010). The levels of miR156 gradually decrease with age, while in turn the expression of its target *SPL* genes increases. The miR156-regulated *SPL* genes control a suite of temporal changes during development including transition from the juvenile to adult phase (Wu and Poethig 2006; Wang et al. 2009; Wu et al. 2009; Yamaguchi et al. 2009; Wang and Wang 2015). The switch from vegetative growth to flowering is biphasic depending on gibberellin (Yu et al. 2012; Yamaguchi et al. 2014). Although gibberellin promotes termination of vegetative development, it inhibits flower formation. First, gibberellin levels increase and stimulate production of key flowering factors including LEAFY that stimulates the gibberellin degradation pathway. As gibberellin levels fall, the gibberellin-sensitive DELLA proteins accumulate and directly bind to SPL transcription factors promoting flowering through synergy between LEAFY and APETALA1.

In addition, elevated levels of SPLs negatively regulate the TTG1-dependent biological processes of acropetal anthocyanin accumulation and trichome distribution on the inflorescence stems or floral organs, possibly by interfering with the integrity of a MBW complex (Yu et al. 2010; Gou et al. 2011).

Ectopic expression in *A. thaliana* of the miR156-resistant forms *SPLr4/5*, homologs of *C. creticus SPLA/B*, resulted in the reduction of trichomes on the adaxial surface of cauline leaves. Moreover, the trichome phenotype was correlated with downregulation of *GL2* trichome inducer expression. As *GL2* is the downstream molecular target of MBW, the SPLs most likely modify the complex by recruiting TTG1 and disrupt the TTG1/GL2 developmental signaling pathway that controls trichome formation. It will be of great interest to explore in future work whether the SPLs negatively regulate trichome formation through destabilization of a MBW transcriptional activation complex. Moreover, two conclusions can be drawn given that SPLr4 and SPLr5 interference exclusively affects trichome formation without disturbing root-hair patterning or flavonoids biosynthesis. Firstly, SPL4/5 are not attached on the ternary MBW complex to form a quaternary one to prevent complex binding to *GL2* promoter as *GL2*, which is a negative regulator of root-hair formation, is normally expressed in seedlings. Secondly, upon root-hair morphogenesis and flavonoids biosynthesis MBW complex integrity is retained due to the heterogeneity of MYB and bHLH interacting partners. These heterogeneous factors protect the complex by SPL penetration.

The negative effect of SPLs on trichome formation has been recently enlightened (Xue et al. 2014). Our results show that *SPL4/5* overexpression has a moderately positive effect on the expression of trichome *TCL1* and *TRY* repressor genes, in agreement with previous results on *SPL9* (Yu et al. 2010). However, constitutive expression of *LOST MERISTEMS* (*LOMs*) transcription factors belonging to the GRAS-domain containing family promoted trichome formation. Physical interaction between LOMs and SPLs underpinned the repression of SPL activity. Moreover, microarray data support the opposite expression pattern between especially *SPL4* and *GL2* (Supplementary Fig. 8). While *TTG1* expression is constant during vegetative-to-reproductive phase transition or leaf expansion, the expression of *GL2* progressively decreases contrary to elevated expression of *SPLs*. The data support the notion that the MBW complex is likely modified by SPLs having a major effect on trichome formation.

Nevertheless, the fate of the SPL-TTG1 interaction in *C. creticus* still remains vague. A tantalizing hypothesis is that the SPL-TTG1 hub first terminates trichome development and then initiates terpenes biosynthesis. A remarkable experimental evidence in this context is the progressive regulation of sesquiterpene biosynthesis by miR156-SPLs (Yu et al. 2015). In *Pogostemon cablin*, the age-regulated SPLs are the molecular link between developmental timing and sesquiterpene production. Although very little is known about *C. creticus*, it will be tempting to shed light on SPL-TTG1 function as a check point switch between developmental and biochemical processes.

Acknowledgments This work was supported by PENED 2001-01ED416 and GSRT 09SYN-879 (SysTerp) grants. Results presented in this article were part of EI doctoral thesis. G.D., A.A. and D.T. are indebted for funding to IKY fellowships of excellence for postgraduate studies in Greece-Siemens program.

Author contributions S.R., S.P., P.H., and A.K.K. conceived and designed the experiments. E.I., D.T., G.D., A.M., G.T., A.A., A.A. and D.A. performed the experiments. D.T., G.D., and S.R. analyzed the data. S.R., P.H., and A.K.K. prepared the manuscript with editing from all authors. P.H., and A.K.K. funding acquisition.

References

Balkunde R, Pesch M, Hülskamp M (2010) Trichome patterning in *Arabidopsis* thaliana from genetic to molecular models. Curr Top Dev Biol 91:299–321

Balkunde R, Bouyer D, Hülskamp M (2011) Nuclear trapping by GL3 controls intercellular transport and redistribution of TTG1 protein in *Arabidopsis*. Development 138:5039–5048

Baudry A, Heim MA, Dubreucq B, Caboche M, Weisshaar B, Lepiniec L (2004) TT2, TT8, and TTG1 synergistically specify the expression of BANYULS and proanthocyanidin biosynthesis in *Arabidopsis thaliana*. Plant J 39:366–380

Bernhardt C, Lee MM, Gonzalez A, Zhang F, Lloyd A, Schiefelbein J (2003) The bHLH genes GLABRA3 (GL3) and ENHANCER OF GLABRA3 (EGL3) specify epidermal cell fate in the *Arabidopsis* root. Development 130:6431–6439

Bernhardt C, Zhao M, Gonzalez A, Lloyd A, Schiefelbein J (2005) The bHLH genes GL3 and EGL3 participate in an intercellular regulatory circuit that controls cell patterning in the *Arabidopsis* root epidermis. Development 132:291–298

Birkenbihl RP, Jach G, Saedler H, Huijser P (2005) Functional dissection of the plant-specific SBP-domain: overlap of the DNA binding and nuclear localization domains. J Mol Biol 352:585–596

Bruex A, Kainkaryam RM, Wieckowski Y, Kang YH, Bernhardt C, Xia Y, Zheng X, Wang JY, Lee MM, Benfey P, Woolf PJ, Schiefelbein J (2012) A gene regulatory network for root epidermis cell differentiation in *Arabidopsis*. PLoS Genet 8:e1002446

Cheng Y, Zhu W, Chen Y, Ito S, Asami T, Wang X (2014) Brassinosteroids control root epidermal cell fate via direct regulation of a MYB-bHLH-WD40 complex by GSK3-like kinases. Elife 3:e02525

Costa S, Shaw P (2006) Chromatin organization and cell fate switch respond to positional information in *Arabidopsis*. Nature 439:493–496

Daras G, Rigas S, Penning B, Milioni D, McCann MC, Carpita NC, Fasseas C, Hatzopoulos P (2009) The thanatos mutation in *Arabidopsis thaliana* cellulose synthase 3 (AtCesA3) has a dominant-negative effect on cellulose synthesis and plant growth. New Phytol 184:114–126

Daras G, Rigas S, Tsitsekian D, Zur H, Tuller T, Hatzopoulos P (2014) Alternative transcription initiation and the AUG context configuration control dual-organellar targeting and functional competence of *Arabidopsis* Lon1 protease. Mol Plant 7:989–1005

Di Cristina M, Sessa G, Dolan L, Linstead P, Baima S, Ruberti I, Morelli G (1996) The *Arabidopsis* Athb-10 (GLABRA2) is an HD-Zip protein required for regulation of root hair development. Plant J 10:393–402

Esch JJ, Chen MA, Hillestad M, Marks MD (2004) Comparison of TRY and the closely related At1g01380 gene in controlling *Arabidopsis* trichome patterning. Plant J 40:860–869

Falara V, Fotopoulos V, Margaritis T, Anastasaki T, Pateraki I, Bosabalidis AM, Kafetzopoulos D, Demetzos C, Pichersky E, Kanellis AK (2008) Transcriptome analysis approaches for the isolation of trichome-specific genes from the medicinal plant *Cistus creticus* subsp. creticus. Plant Mol Biol 68:633–651

Falara V, Pichersky E, Kanellis AK (2010) A copal-8-ol diphosphate synthase from the angiosperm *Cistus creticus* subsp. creticus is a putative key enzyme for the formation of pharmacologically active, oxygen-containing labdane-type diterpenes. Plant Physiol 154:301–310

Galway ME, Masucci JD, Lloyd AM, Walbot V, Davis RW, Schiefelbein JW (1994) The TTG gene is required to specify epidermal cell fate and cell patterning in the Arabidopsis root. Dev Biol 166:740–754

Gietz D, St Jean A, Woods RA, Schiestl RH (1992) Improved method for high efficiency transformation of intact yeast cells. Nucleic Acids Res 20:1425

Gonzalez A, Zhao M, Leavitt JM, Lloyd AM (2008) Regulation of the anthocyanin biosynthetic pathway by the TTG1/bHLH/Myb transcriptional complex in *Arabidopsis* seedlings. Plant J 53:814–827

Gou JY, Felippes FF, Liu CJ, Weigel D, Wang JW (2011) Negative regulation of anthocyanin biosynthesis in *Arabidopsis* by a miR156-targeted SPL transcription factor. Plant Cell 23:1512–1522

Hulskamp M, Schnittger A, Folkers U (1999) Pattern formation and cell differentiation: trichomes in *Arabidopsis* as a genetic model system. Int Rev Cytol 186:147–178

Ishida T, Kurata T, Okada K, Wada T (2008) A genetic regulatory network in the development of trichomes and root hairs. Annu Rev Plant Biol 59:365–386

Johnson HB (1975) Plant pubescence-Ecological perspective. Bot Rev 41:233–258

Kirik V, Simon M, Huelskamp M, Schiefelbein J (2004) The ENHANCER OF TRY AND CPC1 gene acts redundantly with TRIPTYCHON and CAPRICE in trichome and root hair cell patterning in *Arabidopsis*. Dev Biol 268:506–513

Kirik V, Lee MM, Wester K, Herrmann U, Zheng Z, Oppenheimer D, Schiefelbein J, Hulskamp M (2005) Functional diversification of MYB23 and GL1 genes in trichome morphogenesis and initiation. Development 132:1477–1485

Lee MM, Schiefelbein J (1999) WEREWOLF, a MYB-related protein in *Arabidopsis*, is a position-dependent regulator of epidermal cell patterning. Cell 99:473–483

Li S (2014) Transcriptional control of flavonoid biosynthesis: fine-tuning of the MYB-bHLH-WD40 (MBW) complex. Plant Signal Behav 9:e27522

Masucci JD, Rerie WG, Foreman DR, Zhang M, Galway ME, Marks MD, Schiefelbein JW (1996) The homeobox gene GLABRA2 is required for position-dependent cell differentiation in the root epidermis of *Arabidopsis thaliana*. Development 122:1253–1260

Mehrtens F, Kranz H, Bednarek P, Weisshaar B (2005) The *Arabidopsis* transcription Factor MYB12 Is a flavonol-specific regulator of phenylpropanoid biosynthesis. Plant Physiol 138:1083–1096

Papaefthimiou D, Papanikolaou A, Falara V, Givanoudi S, Kostas S, Kanellis AK (2014) Genus *Cistus*: a model for exploring labdane-type diterpenes' biosynthesis and a natural source of high value products with biological, aromatic, and pharmacological properties. Front Chem 2:35

Pateraki I, Kanellis AK (2004) Isolation of high-quality nucleic acids from *Cistus creticus* ssp. creticus and other medicinal plants. Anal Biochem 328:90–92

Payne CT, Zhang F, Lloyd AM (2000) GL3 encodes a bHLH protein that regulates trichome development in *Arabidopsis* through interaction with GL1 and TTG1. Genetics 156:1349–1362

Poustka F, Irani NG, Feller A, Lu Y, Pourcel L, Frame K, Grotewold E (2007) A trafficking pathway for anthocyanins overlaps with the endoplasmic reticulum-to-vacuole protein-sorting route in *Arabidopsis* and contributes to the formation of vacuolar inclusions. Plant Physiol 145:1323–1335

Rigas S, Daras G, Laxa M, Marathias N, Fasseas C, Sweetlove LJ, Hatzopoulos P (2009) The role of Lon1 protease in post-germinative growth and maintenance of mitochondrial function in *Arabidopsis thaliana*. New Phytol 181:588–600

Sambrook J, Fritsch EF, Maniatis T (1989) Molecular cloning: a laboratory manual 2nd edn, Cold Spring Harbor Laboratory Press, New York

Schellmann S, Schnittger A, Kirik V, Wada T, Okada K, Beermann A, Thumfahrt J, Jürgens G, Hülskamp M (2002) TRIPTYCHON and CAPRICE mediate lateral inhibition during trichome and root hair patterning in *Arabidopsis*. EMBO J 21:5036–5046

Schiefelbein J, Kwak SH, Wieckowski Y, Barron C, Bruex A (2009) The gene regulatory network for root epidermal cell-type pattern formation in Arabidopsis. J Exp Bot 60:1515–1521

Schiefelbein J, Huang L, Zheng X (2014) Regulation of epidermal cell fate in Arabidopsis roots: the importance of multiple feedback loops. Front Plant Sci 5:47

Schnittger A, Folkers U, Schwab B, Jurgens G, Hulskamp M (1999) Generation of a spacing pattern: the role of triptychon in trichome patterning in Arabidopsis. Plant Cell 11:1105–1116

Simon M, Lee MM, Lin Y, Gish L, Schiefelbein J (2007) Distinct and overlapping roles of single-repeat MYB genes in root epidermal patterning. Dev Biol 311:566–578

Simon M, Bruex A, Kainkaryam RM, Zheng X, Huang L, Woolf PJ, Schiefelbein J (2013) Tissue-specific profiling reveals transcriptome alterations in *Arabidopsis* mutants lacking morphological phenotypes. Plant Cell 25:3175–3185

Szymanski DB, Jilk RA, Pollock SM, Marks MD (1998) Control of GL2 expression in *Arabidopsis* leaves and trichomes. Development 125:1161–1171

Tominaga R, Iwata M, Okada K, Wada T (2007) Functional analysis of the epidermal-specific MYB genes CAPRICE and WEREWOLF in *Arabidopsis*. Plant Cell 19:2264–2277

Tominaga-Wada R, Ishida T, Wada T (2011) New insights into the mechanism of development of *Arabidopsis* root hairs and trichomes. Int Rev Cell Mol Biol 286:67–106

Wada T, Tachibana T, Shimura Y, Okada K (1997) Epidermal cell differentiation in *Arabidopsis* determined by a Myb homolog, CPC. Science 277:1113–1116

Walker AR, Davison PA, Bolognesi-Winfield AC, James CM, Srinivasan N, Blundell TL, Esch JJ, Marks MD, Gray JC (1999) The TRANSPARENT TESTA GLABRA1 locus, which regulates trichome differentiation and anthocyanin biosynthesis in *Arabidopsis*, encodes a WD40 repeat protein. Plant Cell 11:1337–1350

Walter M, Chaban C, Schütze K, Batistic O, Weckermann K, Näke C, Blazevic D, Grefen C, Schumacher K, Oecking C, Harter K, Kudla J (2004) Visualization of protein interactions in living plant cells using bimolecular fluorescence complementation. Plant J 40:428–438

Wang H, Wang H (2015) The miR156/SPL Module, a regulatory hub and versatile toolbox, gears up crops for enhanced agronomic traits. Mol Plant 8:677–688

Wang JW, Czech B, Weigel D (2009) miR156-regulated SPL transcription factors define an endogenous flowering pathway in *Arabidopsis thaliana*. Cell 138:738–749

Wu G, Poethig RS (2006) Temporal regulation of shoot development in *Arabidopsis thaliana* by miR156 and its target SPL3. Development 133:3539–3547

Wu G, Park MY, Conway SR, Wang JW, Weigel D, Poethig RS (2009) The sequential action of miR156 and miR172 regulates developmental timing in *Arabidopsis*. Cell 138:750–759

Xing S, Salinas M, Höhmann S, Berndtgen R, Huijser P (2010) miR156-targeted and nontargeted SBP-box transcription factors act in concert to secure male fertility in *Arabidopsis*. Plant Cell 22:3935–3950

Xu W, Dubos C, Lepiniec L (2015) Transcriptional control of flavonoid biosynthesis by MYB-bHLH-WDR complexes. Trends Plant Sci 20:176–185

Xue XY, Zhao B, Chao LM, Chen DY, Cui WR, Mao YB, Wang LJ, Chen XY (2014) Interaction between two timing microRNAs controls trichome distribution in *Arabidopsis*. PLoS Genet 10:e1004266

Yamaguchi A, Wu MF, Yang L, Wu G, Poethig RS, Wagner D (2009) The microRNA-regulated SBP-Box transcription factor SPL3 is a direct upstream activator of LEAFY, FRUITFULL, and APETALA1. Dev Cell 17:268–278

Yamaguchi N, Winter CM, Wu MF, Kanno Y, Yamaguchi A, Seo M, Wagner D (2014) Gibberellin acts positively then negatively to control onset of flower formation in *Arabidopsis*. Science 344:638–641

Yu N, Cai WJ, Wang S, Shan CM, Wang LJ, Chen XY (2010) Temporal control of trichome distribution by microRNA156-targeted SPL genes in *Arabidopsis thaliana*. Plant Cell 22:2322–2335

Yu S, Galvão VC, Zhang YC, Horrer D, Zhang TQ, Hao YH, Feng YQ, Wang S, Schmid M, Wang JW (2012) Gibberellin regulates the *Arabidopsis* floral transition through miR156-targeted SQUAMOSA promoter binding-like transcription factors. Plant Cell 24:3320–3332

Yu ZX, Wang LJ, Zhao B, Shan CM, Zhang YH, Chen DF, Chen XY (2015) Progressive regulation of sesquiterpene biosynthesis in *Arabidopsis* and *Patchouli* (*Pogostemon cablin*) by the miR156-targeted SPL transcription factors. Mol Plant 8:98–110

Zhang F, Gonzalez A, Zhao M, Payne CT, Lloyd A (2003) A network of redundant bHLH proteins functions in all TTG1-dependent pathways of Arabidopsis. Development 130:4859–4869

Zhao M, Morohashi K, Hatlestad G, Grotewold E, Lloyd A (2008) The TTG1-bHLH-MYB complex controls trichome cell fate and patterning through direct targeting of regulatory loci. Development 135:1991–1999